Received 12 March 2018
Revised 24 May 2018
Accepted 26 May 2018

Numerical determination of interfacial heat transfer coefficient for an aligned dual scale porous medium

Safa Sabet
Izmir Yuksek Teknoloji Enstitusu, Urla, Turkey

Moghtada Mobedi
Izmir Institute of Technology, Izmir, Turkey

Murat Barisik
Izmir Yuksek Teknoloji Enstitusu, Urla, Turkey, and

Akira Nakayama
Shizuoka University, Shizuoka, Japan

Abstract

Purpose – Fluid flow and heat transfer in a dual scale porous media is investigated to determine the interfacial convective heat transfer coefficient, numerically. The studied porous media is a periodic dual scale porous media. It consists of the square rods which are permeable in an aligned arrangement. It is aimed to observe the enhancement of heat transfer through the porous media, which is important for thermal designers, by inserting intra-pores into the square rods. A special attention is given to the roles of size and number of intra-pores on the heat transfer enhancement through the dual scale porous media. The role of intra-pores on the pressure drop of air flow through porous media is also investigated by calculation and comparison of the friction coefficient.

Design/methodology/approach – To calculate the interfacial convective heat transfer coefficient, the governing equations which are continuity, momentum and energy equations are solved to determine velocity, pressure and temperature fields. As the dual scale porous structure is periodic, a representative elementary volume is generated, and the governing equations are numerically solved for the selected representative volume. By using the obtained velocity, pressure and temperature fields and using volume average definition, the volume average of aforementioned parameters is calculated and upscaled. Then, the interfacial convective heat transfer coefficient and the friction coefficient is numerically determined. The interparticle porosity is changed between 0.4 and 0.75, while the intraparticle varies between 0.2 and 0.75 to explore the effect of intra-pore on heat transfer enhancement.

Findings – The obtained Nusselt number values are compared with corresponding mono-scale porous media, and it is found that heat transfer through a porous medium can be enhanced threefold (without the increase of pressure drop) by inserting intraparticle pores in flow direction. For the porous media with low values of interparticle porosity (i.e. = 0.4), an optimum intraparticle porosity exists for which the highest heat transfer enhancement can be achieved. This value was found around 0.3 when the interparticle porosity was 0.4.

Research limitations/implications – The results of the study are interesting, especially from heat transfer enhancement point of view. However, further studies are required. For instance, studies should be performed to analyze the rate of the heat transfer enhancement for different shapes and arrangements of particles and a wider range of porosity. The other important parameter influencing heat transfer enhancement is the direction of pores. In the present study, the intraparticle pores are in flow direction; hence, the enhancement rate of heat transfer for different directions of pores must also be investigated.

Practical implications – The application of dual scale porous media is widely faced in daily life, nature and industry. The flowing of a fluid through a fiber mat, woven fiber bundles, multifilament textile fibers, oil filters and fractured porous media are some examples for the application of the heat and fluid flow through a dual scale porous media. Heat transfer enhancement.

International Journal of Numerical Methods for Heat & Fluid Flow
Vol. 28 No. 11, 2018
pp. 2716-2733

0961-5539
DOI 10.1108/HFF-03-2018-0097

Social implications – The enhancement of heat transfer is a significant topic that gained the attention of researchers in recent years. The importance of topic increases day-by-day because of further demands for downsizing of thermal equipment and heat recovery devices. The aim of thermal designers is to enhance heat transfer rate in thermal devices and to reduce their volume (and/or weight in some applications) by using lower mechanical power for cooling.

Originality/value – The present study might be the first study on determination of thermal transport properties of dual scale porous media yielded interesting results such as considerable enhancement of heat transfer by using proper intraparticle channels in a porous medium.

Keywords Porous media, Inter and intraparticle porosity, Numerical heat transfer, Interfacial convective heat transfer coefficient, Numerical determination

Paper type Research paper

Nomenclature

A_{sf} = Interfacial area between solid and fluid phases (m^2);
A_{ss} = Specific solid–fluid interface area (m^2/m^3);
c_p = Specific heat of fluid (J/kgK);
D = Height of intraparticle pore, m;
D = Size of square particle, m;
H = Dimension of structural unit (REV), m;
h_{sf} = Interfacial convective heat transfer coefficient (W/m^2K);
k_f = Thermal conductivity of fluid (W/mK);
L = Length, m;
Nu = interfacial Nusselt number;
P = Pressure, Pa;
Pr = Prandtl number;
Re = Reynolds number;
T = Temperature (K);
U = Velocity in x direction, m/s;
$\overrightarrow{u}$ = Velocity vector, m/s;
u_D = Darcian velocity, m/s;
V = Velocity in y-direction, m/s; and
V = Volume, m^3.

Greek symbols

A = Thermal diffusivity of fluid (m^2/s);
E = Porosity;
M = Dynamic viscosity, Ns/m^2;
N = Kinematic viscosity, m^2/s; and
P = Density, kg/m^3.

Subscripts

b = Bulk;
f = Fluid;
p = Particle; and
xx = Longitudinal.

1. Introduction

The application of dual scale porous media is widely faced in daily life, nature and industry. The flowing of a fluid through a fiber mat, woven fiber bundles, multifilament textile fibers,

oil filters and fractured porous media are some examples for the application of the fluid flow through a dual scale porous media. In the case of temperature difference between flowing fluid and porous structure (such as drying of a wet thick fiber mat), the energy equations for the porous structure and fluid should be added into the motion equations.

A dual scale porous medium is a porous structure in which the solid region is also permeable since there are pores in the solid in which fluid can flow. A schematic view of a dual scale porous media is shown in Figure 1. As illustrated, there are two kinds of pores in a dual scale porous medium. The first type, known as interparticle pore, is the main pore of the porous structure and exists between the particles. The second type called intraparticle pore exists within the particles since the particles are permeable. Furthermore, three types of porosities can be defined for a dual scale porous media as interparticle, intraparticle and bulk porosities. These porosities can be defined by following equalities:

$$\varepsilon_p = \frac{V_{vp}}{V_p};\ \ \varepsilon_f = \frac{V_{vf}}{V_t};\ \ \varepsilon_t = \frac{V_{vt}}{V_t} \tag{1}$$

Where ε_f, ε_p and ε_t are the interparticle, intraparticle and bulk porosities, respectively. The volumes of interparticle, intraparticle and total pores are shown by V_{vf}, V_{vp} and V_{vt} respectively. Furthermore, V_p and V_t are the total volumes of solid phase and dual scale porous media. The size of interparticle pores is generally greater than the intraparticle pores and consequently, the interparticle porosity is generally greater than the intraparticle porosity. The inter- and intraparticle pores are also called as macro and micro pores by some researchers (Yu and Cheng, 2002). The fluid flow in a dual scale porous medium can also be classified into two types as inter- and intraparticle flows.

The mechanism of heat and fluid flow in porous media is complex due to the existence of different phases and it is difficult to obtain the exact temperature, velocity and pressure fields for the entire porous medium. The application of macroscopic method can overcome difficulties, such as the complexity of the flow in the pores, discontinuity of the flow field, differences in the thermophysical properties of phases (Ingham and Pop, 2005). On the other hand, the application of the macroscopic method requires knowledge of the macroscopic transport properties of the studied porous medium, such as permeability and interfacial heat transfer coefficient (Celik *et al.*, 2017). These transport properties can be determined experimentally or theoretically. The continuity, momentum and energy equations can be solved for the pore level of a porous medium and then the macroscopic transport parameters, such as permeability, interfacial convective heat transfer coefficient and thermal dispersion conductivity can be obtained by using volume average technique.

Improvements in computer and software technologies facilitate the computational determination of the interfacial convective heat transfer coefficient for a porous medium. Periodic porous media can be easily modeled using a computer, while techniques such as

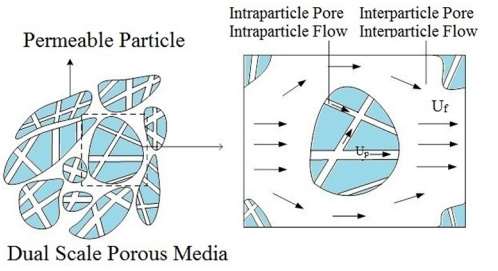

Figure 1.
Schematic view of a dual scale porous medium

tomography can be employed to obtain a digital representation of a heterogeneous porous medium with complex pore structure. An example study for determining interfacial convective heat transfer coefficient with a pore scale computational approach is the study of Kuwahara *et al.* (2000), who studied the heat and fluid flow between isothermal square rods with a staggered arrangement under thermally non-equilibrium condition. A correlation for the Nusselt number was proposed for a wide range of porosity, Prandtl and Reynolds numbers. Saito and de Lemos (2005) also determined the interfacial heat transfer coefficient numerically for an infinite porous medium in which fully developed flow condition is valid. Furthermore, Ozgumus and Mobedi (2014) investigated the effects of the pore to throat size ratio on the interfacial heat transfer coefficient for a periodic porous media containing an in-line array of rectangular rods numerically. The study was performed for the pore to throat size ratios between 1.63 and 7.46, porosities from 0.7 to 0.9 and Reynolds numbers between 1 and 100. It was observed that in addition to porosity and Reynolds number, the parameter of the pore to throat size ratio plays an important role in the heat transfer in porous media.

An extensive literature survey on determining macroscopic transport properties in porous media showed that numerous studies on determination of permeability in a dual scale porous media were conducted. Those studies were summarized by Sabet and Mobedi (2016). However, to the best of our knowledge, no study has been done to determine interfacial heat transfer coefficients through dual scaled porous media. The value of interfacial heat transfer coefficient for local non-thermal equilibrium heat transfer is a requirement should be known accurately. This lack of knowledge motivated the authors to do the present study to have an idea about the value of the interfacial heat transfer coefficient and to investigate the variation of this coefficient with different geometrical and flow parameters.

In this study, the interfacial convective heat transfer coefficient of porous media consisting of the square rods with different values of interparticle and intraparticle porosity are examined numerically to determine the effects of both types of porosities on the interfacial heat transfer coefficient between the solid and fluid. Furthermore, the pressure drop through the porous medium is calculated and then, the enhancement of heat transfer and change of pressure drop through the porous media is measured by inserting intraparticle pores in the solid particles. The present study might be the first study on determination of thermal transport properties of a dual scale porous media yielded interesting results such a considerable enhancement of heat transfer by using proper intraparticle channels in a porous medium.

2. The considered dual scale porous media

The geometry of the considered porous media and representative elementary volume (REV) are shown in Figure 2. A periodical REV with the dimensions of H $\times$ H is chosen as the computational domain. The flow in the REV is assumed fully developed and periodical. The permeable square particles are placed with an in-line arrangement. The number of symmetrical intraparticle pores is two in longitudinal flow direction for the entire present study. The height of the intraparticle pore is shown by "d" and changes from 0.2D to 0.75D, where D is the size of a square particle. The interparticle porosity is changed between 0.4 and 0.75 while the intraparticle porosity varies between 0.2 and 0.75. The fluid flowing through the medium is assumed to be Newtonian and incompressible with constant thermophysical properties. The flow is laminar and the study is performed for air with a density of 1.225 kg/m^3 and dynamics viscosity of 1.7894×10^{-5} kg/ms. The calculations are performed for the pore scaled Reynolds number between 50 and 600.

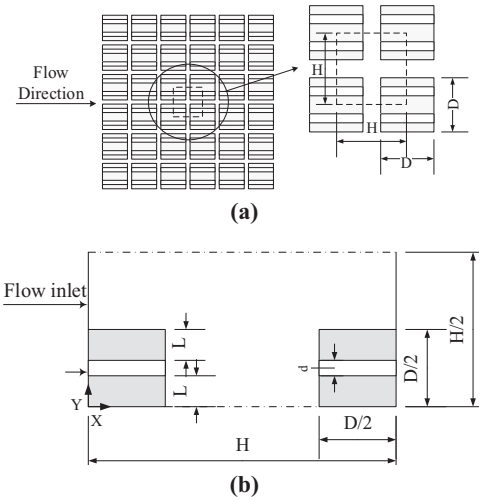

Figure 2.
The studied dual scale porous medium a) general view and b) computational domain

3. Governing equations and boundary conditions for determination of interfacial convective heat transfer coefficient

The fluid flow in inter- and intra-particle pores is assumed incompressible and steady. The continuity and momentum equations are solved to determine the velocity and pressure distributions in the pores. These equations in Cartesian coordinate can be written as follows:

$$\frac{\partial u}{\partial x} + \frac{\partial v}{\partial y} = 0 \tag{2}$$

$$u\frac{\partial u}{\partial x} + v\frac{\partial u}{\partial y} = -\frac{1}{\rho}\frac{\partial p}{\partial x} + \nu\left(\frac{\partial^2 u}{\partial x^2} + \frac{\partial^2 u}{\partial y^2}\right) \tag{3}$$

$$u\frac{\partial v}{\partial x} + v\frac{\partial v}{\partial y} = -\frac{1}{\rho}\frac{\partial p}{\partial y} + \nu\left(\frac{\partial^2 v}{\partial x^2} + \frac{\partial^2 v}{\partial y^2}\right) \tag{4}$$

where u and v are the velocity components in x and y directions and p is the pressure. ρ and ν are density and kinematic viscosity of fluid, respectively.

The energy equation for the fluid and solid phases should be solved to determine the temperature distribution in entire porous media and then find the interfacial convective heat transfer coefficient.

$$\rho_f c_{pf}\left(u\frac{\partial T}{\partial x} + v\frac{\partial T}{\partial y}\right) = k_f\left(\frac{\partial^2 T}{\partial x^2} + \frac{\partial^2 T}{\partial y^2}\right) \tag{5}$$

$$\frac{\partial^2 T}{\partial x^2} + \frac{\partial^2 T}{\partial y^2} = 0 \tag{6}$$

For a particle in porous media, the pore scale Biot number can be defined as follows:

$$Bi = \frac{h_{sf} l}{k_s} \tag{7}$$

Where h_{sf}, l and k_s are defined as solid-fluid surface interfacial heat transfer coefficient, characteristic length of particle and thermal conductivity of solid phase. The value of l (particle size in this study) is small and k_s is high for many solids in practical applications such as metals (in metal foams) and stones (in rock). Hence, B_i number takes small values (i.e. $B_i \ll 1$) permitting researchers to apply constant temperature assumptions for solid phase. Hence, there might be no need to solve the heat conduction equation for solid (Celik *et al.*, 2017).

To solve equations (2-5), the boundary conditions for velocities and temperature at the boundaries of REVs and at the fluid-solid interfaces are necessary. As Figure 2(b) shows, the boundary conditions for the microscopic equations are chosen as symmetry for the top and the bottom of the REV. The velocity and temperature gradients at the fluid outlet boundary are zero; therefore, no diffusion transport exists. Finally, the periodic velocity and temperature profiles are generated for the inlet and outlet boundaries. The employed boundary conditions in a mathematical statement can be written as follows: On the solid walls:

$$u = v = 0, T_s = \text{Constant} \tag{8}$$

On the fluid-solid interfaces:

$$T = T_s \tag{9}$$

For the top and the bottom boundaries:

$$\frac{\partial u}{\partial y} = \frac{\partial v}{\partial y} = \frac{\partial T}{\partial y} = 0 \tag{10}$$

For the inlet boundary:

$$u = f(y), T = g(y) \tag{11}$$

For the outlet boundary:

$$\frac{\partial u}{\partial x} = \frac{\partial v}{\partial x} = \frac{\partial T}{\partial x} = 0 \tag{12}$$

The method for periodic boundary conditions of motion and heat transfer equations for the considered REV (determination of f (y) and g (y)) are described in the next section. For a quantity in a REV shown with the volume of V, two following types of volume averaging exist:

$$\langle \phi \rangle = \frac{1}{V} \int_V \phi \, dV \tag{13}$$

$$\langle \phi \rangle^x = \frac{1}{V_x} \int_{V_x} \phi \, dV \tag{14}$$

which are called as volume average and intrinsic volume average of ϕ quantity, respectively. By using these definitions and applying them to the pore scale energy equation for solid and fluid, and doing some mathematical manipulation, the steady-state volume averaged energy equation for solid and fluid can be yielded as follows:

$$\varepsilon \rho_f c_{p_f} \left(\langle u \rangle \frac{\partial \langle T \rangle^f}{\partial x^2} + \langle v \rangle \frac{\partial \langle T \rangle^f}{\partial y^2} \right) = \left(k_{stag,f} + \varepsilon k_{disp} \right) \left(\frac{\partial^2 \langle T \rangle^f}{\partial x^2} + \frac{\partial^2 \langle T \rangle^f}{\partial y^2} \right) + h_v \left(\langle T \rangle^s - \langle T \rangle^f \right) \tag{15}$$

$$\left(k_{stag,s} \right) \frac{\partial^2 \langle T \rangle^s}{\partial x^2} + \frac{\partial^2 \langle T \rangle^s}{\partial y^2} - h_v \left(\langle T \rangle^s - \langle T \rangle^f \right) = 0 \tag{16}$$

where $\langle T \rangle^s$ and $\langle T \rangle^f$ are volume averaged solid and fluid temperatures. If the pore scale energy equation (5) and volume averaged equation, i.e. equation (15) for fluid are compared, it can be seen, there are three new coefficients energy equation as stagnant thermal conductivity (i.e. $k_{stag,f}$) thermal dispersion conductivity(i.e. k_{disp}) and interfacial heat transfer coefficient (i.e. h_v). Similarly, there are two new coefficients in the volume averaged energy equation for solid equation (15) as stagnant thermal conductivity for solid (i.e. $k_{stag,s}$) and the same interfacial heat transfer coefficient (i.e. h_v). It should be mentioned that stagnant thermal conductivity involves material thermal conductivity (εk_f for fluid phase and $(1-\varepsilon)k_s$ for solid phase) and the effect of thermal tortuosity (k_{tort}). Hence, to find the volume averaged temperature, stagnant and dispersion thermal conductivity and interfacial heat transfer coefficient should be known. The present paper studies the numerical determination of the interfacial heat transfer coefficient and dispersion thermal conductivity for dual scale porous media.

Discussions on the above terms have been performed in details in the study of Ozgumus *et al.* (2013). As it was mentioned above, the final term in equations (15) and (16) refers heat transfer between solid and fluid phases in porous media. To determine its value, the interfacial convective heat transfer coefficient between solid and fluid is defined:

$$h_{sf} = \frac{\int_{A_{sf}} k_f \nabla T_f \cdot \vec{n} \, dA}{A_{sf} \left(\langle T \rangle^s - \langle T \rangle^f \right)} \tag{17}$$

Where h_{sf} is the interfacial convective heat transfer coefficient, A_{sf} is the solid-fluid interface area.

It should be mentioned that there are two definitions of interfacial heat transfer coefficient as surface area based (h_{sf} (W/m^2K)) and volumetric based hv (W/m^3K). The relation between them is given in the equation as follows:

$$h_v = A_{ss} h_{sf} \tag{18}$$

Where A_{ss} is the volumetric surface area and is defined as $A_{ss} = A_{sf}/V$. In this study, there are two types of the surface areas, i.e. the inter- and intra-particle surface area. The effect of them on heat transfer area might be different. In some cases, intraparticle surface area may not have any effect while for some structures its effect might be considerable. This concept must be studied well; however, in this work, the interfacial heat transfer coefficient based on the total area is selected to analyze. The interfacial Nusselt number can also be defined as follows:

$$Nu = \frac{h_{sf} H}{k_f} \tag{19}$$

As can be seen from equation (19) in this study, the dimension of the REV (i.e. H) is selected as characteristic length to define Nusselt number. The same behavior is also observed in numerous other reported studies (Kuwahara *et al.*, 2000, Ozgumus and Mobedi, 2014). Furthermore, to compare the Nusselt number of dual scale with mono-scaled porosity,

equation (19) is modified. The Nusselt number of equation (19) involves the total area of the dual scaled porous media. This area is different from the area of mono-scaled porosity porous media. The comparison of them may not provide a correct idea about the enhancement heat transfer, that is why the heat transfer coefficient of dual scaled porous media should be revised based on the heat transfer area of the corresponding mono-scaled porous structure with the same particle dimension and interparticle porosity.

$$Nu^* = \frac{h^*_{sf} H}{k_f} \tag{20}$$

where h^*_{sf} is the modified heat transfer coefficient based on the area of corresponding mono-scaled porous structure. Pressure drop calculations are also studied since the power needed by a fan (or pump) directly depends on pressure drop. To achieve an opinion about the pressure drop in the channel, the definition of the friction factor is used. Friction factor for considered REV with Darcy velocity of u_m can be defined as:

$$f = \frac{2\Delta P/H}{\frac{1}{2}\rho\, u_m^2} \tag{21}$$

Where $\Delta P/H$ shows pressure drop along the REV (i.e. average pressure difference between inlet and outlet of REV).

4. Numerical procedure and computational details

The pore level heat and fluid flow equations are solved for the considered REV Figure 2(b). The number of grids is chosen as 400 × 400 for the entire domain. A commercial code based on finite volume method is used to solve the governing equations, computationally. The power law scheme is employed to treat the discretization of the convection terms in the momentum equation. The SIMPLE method is used for handling the pressure-velocity coupling. The approximate errors (i.e. residuals) are set to 10^{-9} and 10^{-12} for flow variables and temperature, respectively. As can be seen from Figure 3, the grid independency study is done for two-dimensional dual scale porous medium sample with $\varepsilon_f = 0.75$, $\varepsilon_p = 0.2$ and Re = 100 is displayed and, the discretization with grid number of 160,000 is sufficient to achieve acceptable results.

4.1 Iterative procedure for obtaining periodical fluid flow boundaries

The function f (y) equation (11) provides hydraulic periodicity for the inlet and outlet boundaries of the considered REV. The employed iterative procedure is described in

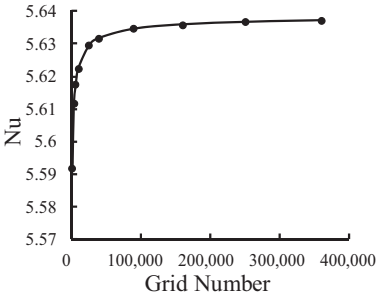

Figure 3.
The change of Nu number with grid number for a dual scale porous media $\varepsilon_f = 0.75$ and $\varepsilon_p = 0.2$ when Re = 100

Figure 4(a) showing the inlet and outlet velocity profiles obtained for determination of velocity profile. Firstly, a uniform velocity profile is assumed. Secondly, after solving the governing equations and obtaining the velocity field, the outlet velocity profile of the first run is used as the inlet boundary condition for the second run and the problem is solved again. This iteration continues until the identical velocity profiles at the inlet and outlet boundaries are achieved and the periodicity of the velocity field could be attained.

4.2 Iterative procedure for obtaining periodical thermal boundaries

As seen in Figure 4(b), to compute the interfacial convective heat transfer coefficient, periodical temperature boundaries should be subsisted at the inlet and outlet boundaries of the REV because of the infinite periodical structure of porous medium and fully developed condition. The temperature profile function g(y) assigned at the inlet fluid boundary can provide thermal periodicity. This function is found by the accompanying technique;

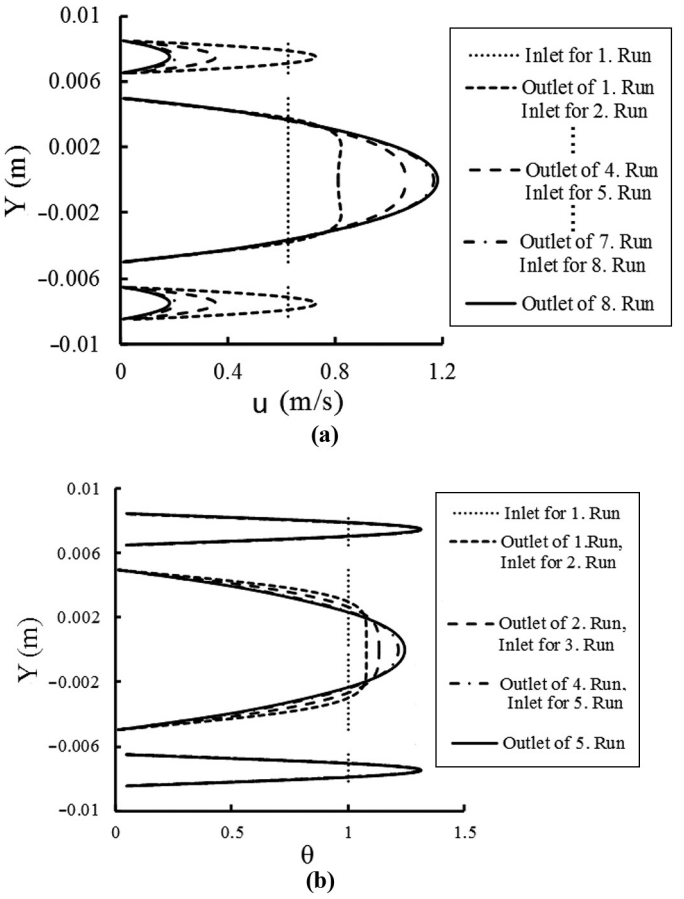

Figure 4.
The change of velocity and temperature profiles at the inlet and outlet of REV to obtain fully developed condition for Re = 600; $\varepsilon_f = 0.75$; and $\varepsilon_p = 0.4$, a) periodic velocity profile and b) periodic temperature profiles

- Toward the start of this iterative procedure, a uniform temperature, different from the solid temperature is defined for the fluid inlet boundary.
- The temperature field for the complete fluid space is acquired by solving the energy equation for fluid.
- The temperature profile for the inlet of the next computation is determined from the dimensionless temperature profile at the outlet boundary of the previous iteration.
- The iterative process will be terminated when the dimensionless temperature distribution between the inlet and outlet and no variety of the interfacial Nusselt number are observed. Since a thermally, fully developed convection heat transfer is valid, no change of the dimensionless temperature and interfacial convective heat transfer should be observed in the sequential REVs through the flow direction in the porous medium.

The dimensionless temperature is defined by:

$$\theta(y) = \frac{T(y) - T_s}{T_b - T_s} \tag{22}$$

where T_s and T_b are the solid and bulk temperatures, respectively. T_b was defined as follows.

$$T_b = \frac{\int_{D/2}^{H/2} uTdy}{\int_{D/2}^{H/2} udy} \tag{23}$$

5. Results and discussions

Before starting to investigate the effects of inter- and intraparticle porosity on the interfacial convective heat transfer coefficient, some studies on porous structures reported in the literature are selected to approve the validations of our computations. The interfacial convective Nusselt number for the selected porous structure are obtained and compared with the results of the reported studies. The validation is performed for the computation of the interfacial convective heat transfer coefficient by solving the microscopic Navier–Stokes and energy equations for fluid phase. The porous media with square rods in in-line arrangement and porosity of 0.75 is created. After solving the equations, the interfacial Nusselt numbers found for this porous media are compared with the results of Ozgumus and Mobedi (2014), Kuwahara *et al.* (2000), Penha *et al.* (2011) and Gamrat *et al.* (2008) and the comparison is shown in Figure 5. As demonstrated in Figure 5, there is an excellent agreement between the results of the present study and the literature results for an extensive variety of Reynolds number.

To compare different temperature fields, a dimensionless temperature definition is used and defined as follows:

$$\langle \theta \rangle^f = \frac{\langle T \rangle^f - T_{\min}}{T_{\max} - T_{\min}} \tag{24}$$

Where $T_{\min}$ and $T_{\max}$ are the minimum and maximum temperatures in the REV, respectively. The streamlines and temperature distribution contours for $\varepsilon_f = 0.75$, $\varepsilon_p = 0.2$ and 0.75 are shown in Figure 6 for Re = 50 and 600, respectively. As can be seen from Figure 6(a), three flow

paths are observed in REV as the main flow passing through the interparticle region, the secondary flows occur in gaps between the solid particles and finally the fluid flow through the intraparticle area. For the low value of ε_p (i.e. $\varepsilon_p = 0.2$), the flow in intraparticle region is weak; however, a straight and strong main flow in the interparticle region from the inlet to outlet boundary exists as shown in Figure 6(a). The weakness of flow in the intraparticle region causes the secondary flows between the particles in the top and bottom of REV occur. For the same porous structure, the increase of intraparticle porosity increases the flow rate in the intraparticle region and the secondary flow between the particles disappears Figure 6(b). The increase of Reynolds number from 50 to 600 does not change the flow behavior Figure 6(c) and (d). The temperature distribution of the same aforementioned porous structures is shown in the right column of Figure 6 for Re = 50 and 600. For the Re = 50 with $\varepsilon_p = 0.2$, the main interparticle region in the center region of the fluid flow is influenced from upstream. The temperature of fluid in the intraparticle region and in the upper and lower gaps are close to the solid temperature due to weak intraparticle flow and a low Reynolds number. Figure 6(b) shows that by increasing of ε_p, although the intraparticle flow becomes stronger, no significant change is observed in the temperature field due to low Reynolds number (i.e. Re = 50). The temperature of intraparticle region of the left particles is only affected by the main upstream flow. From Figure 6(c) and Figure 6(d), it can be seen that as the Reynold number increases (Re = 600) the convection heat transfer becomes dominant causing the reduction of residence period of the fluid particle in the REV and the influence of temperature inside the voids from the upstream flow. The temperature of intraparticle region of Figure 6(c) is not affected by inlet temperature due to weak intraparticle flow; however, the upstream flow completely changes temperature distribution for the porous structure of Figure 6(d) for which $\varepsilon_p = 0.75$.

In Figure 7, the streamlines and temperature distribution contours for $\varepsilon_f = 0.4$ and the intraparticle porosity as 0.2 and 0.4 are shown. As seen in the streamline of Figure 7 (left column), similar to the streamlines of Figure 6, three types of flow paths are observed in REV. Those flow paths are main flow in the interparticle region, secondary flows between the particles and intraparticle flow inside the particles. The main differences between flow paths of Figure 6 and 7 are:

(1) The main flow enters more to the top and bottom gaps for Re = 50.

(2) Number of secondary flows in the upper and lower gaps increases.

The temperature distribution of Figures 6 and 7 are almost the same. By reducing ε_f to 0.4, the interface area of top and bottom gaps increases, while the volume of voids decreases. That is why most of the fluid intraparticle region of Figure 7 is more affected by the temperature of solid walls.

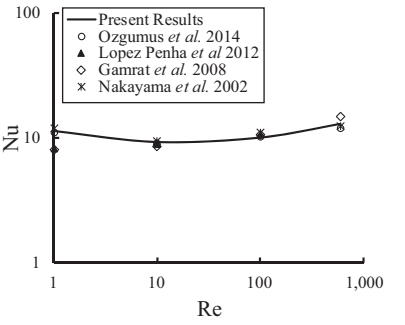

Figure 5.
Comparison of the obtained interfacial Nusselt number with the results of the reported studies

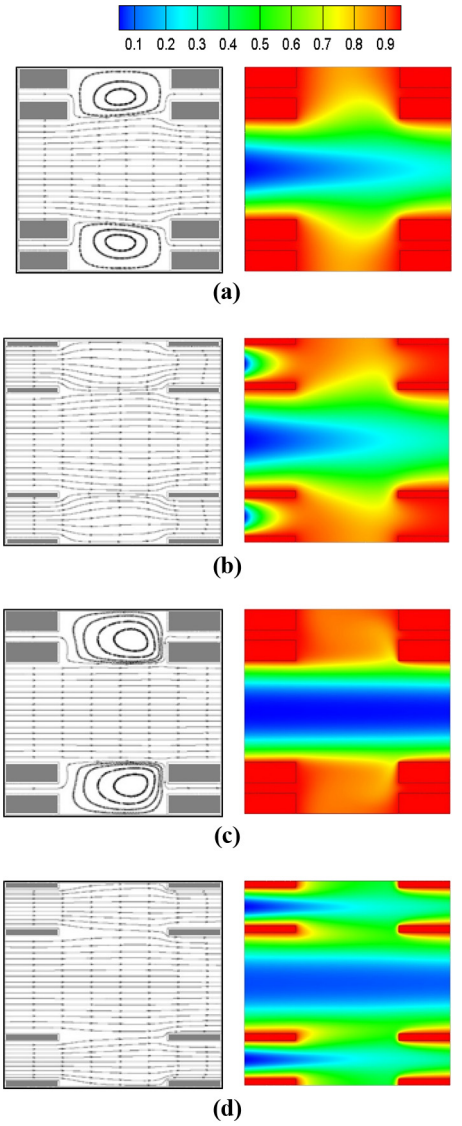

Notes: (a) εp = 0.2, Re = 50; (b) εp = 0.75, Re = 50; (c) εp = 0.2, Re = 600; (d) εp = 0.75, Re = 600

Figure 6.
The streamlines (on the left) and temperature contours (on the right) for dual scale porous media with $\varepsilon_f = 0.75$

The variation of the interfacial Nu with intraparticle porosity for different Re values and three interparticle porosity are shown in Figure 8. As can be seen from the Figure 8(a), the interfacial Nu number increases with ε_p. The rate of increase depends on Re number. For larger values of Re number (e.g. Re = 600), the rate of increase is higher than smaller values

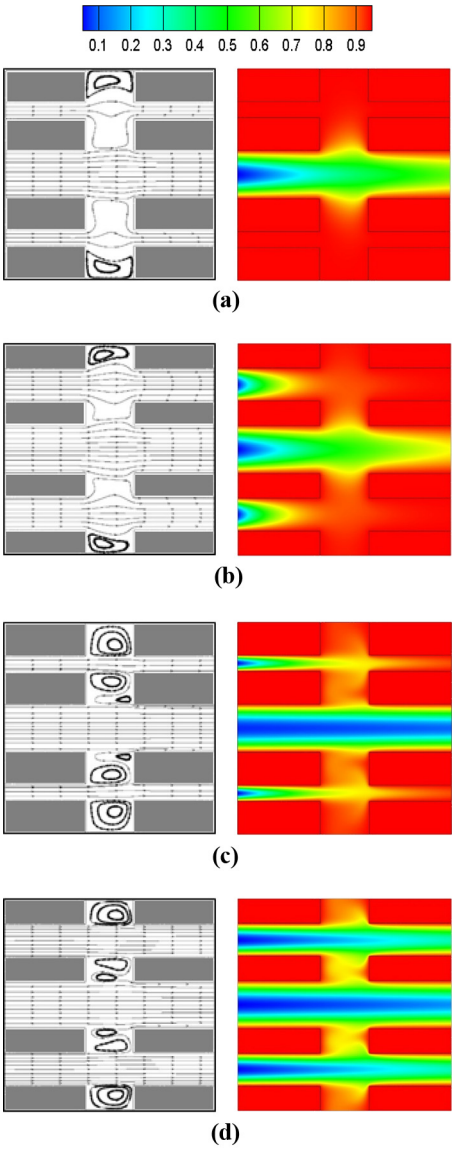

Figure 7.
The streamlines (on the left) and temperature contours (on the right) for dual scale porous media with $\varepsilon_f = 0.4$

Notes: (a) εp = 0.2, Re = 50; (b) εp = 0.4, Re = 50; (c) εp = 0.2, Re = 600; (d) εp = 0.4, Re = 600

of Re number (e.g. Re = 50). The increase of Nu with ε_p can be easily explained because the inactive region between particles in the upper and lower gaps are destroyed by flowing of fluid entering to the intraparticle region. Figure 8(b) represents the interfacial Nu values for the interparticle porosity of 0.6 when ε_p changes between 0.2

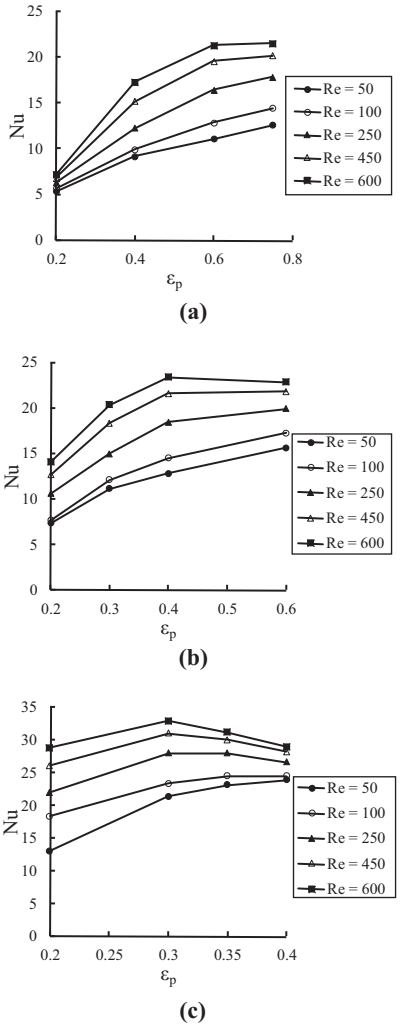

Figure 8.
The variation of Nu number with ε_p for different Re numbers
a) $\varepsilon_f = 0.75$;
b) $\varepsilon_f = 0.6$; and
c) $\varepsilon_f = 0.4$

and 0.6. For Re = 50, 100 and 250, the Nu values increase with the intraparticle porosity. This increase is also observed for Re = 450 and 600 up to $\varepsilon_p = 0.4$, but for the $\varepsilon_p = 0.6$ a slight decrease in Nu value ascertained. In Figure 8(c), the interparticle porosity is 0.4 while the intraparticle porosity again changes between 0.2 and 0.4. An increase of Nu number is observed for Re number of 50 and 100 by an increase of ε_p from 0.2 to 0.3, however, for Re = 250, 450, 600 the decrease of Nu number is observed after $\varepsilon_p = 0.3$. The interfacial heat transfer coefficient is the ratio of heat transfer rate from the surface of the REV to $(T_w - \langle T \rangle^f)$ equation (12). By increasing of Re number, the temperature difference increases due to the strong convective flows in the main interparticle region and it causes a slight decrease in Nusselt number.

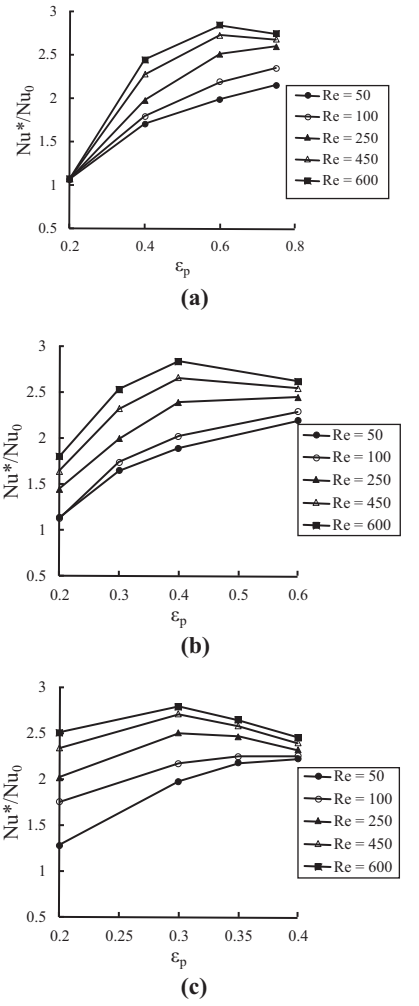

Figure 9.
The ratio of modified Nusselt number* to Nu number of mono-scale porosity porous media a) $\varepsilon_f = 0.75$; b) $\varepsilon_f = 0.6$; and c) $\varepsilon_f = 0.4$

Figure 9 indicates the ratio of modified Nusselt number of dual scale porous media to Nu number of the corresponding (the same intraparticle porosity) mono-scale porous media. In Figure 9, Nu_o represents Nusselt number of the mono-scaled porous media. As can be seen from Figure 9(a), the ratio of Nu numbers for $\varepsilon_p = 0.2$ are almost the same for all studied cases and are near unity. The rate of heat transfer enhancement increases by increasing the Reynolds number and intraparticle porosity due to destroying the secondary flows in the top and bottom gaps of the REV. It is clear that if the value of (Nu^*/Nu_o) is greater than 1, the enhancement of heat transfer exists. This enhancement for $\varepsilon_p = 0.6$ reaches 200 per cent (or 3 times) which is very high value. For low values of the interparticle porosity = 0.6 ($\varepsilon_f = 0.6$ and $\varepsilon_f = 0.4$, Figures 9(b) and (c)), the significant of the intraparticle porosity increases when $\varepsilon_p < 0.4$. For the low values of intraparticle porosity as $\varepsilon_p = 0.2$, the rate of heat transfer enhancement considerably changes with Reynolds number. The interesting point of

Figures 9 (b) and (c) is that the rate of heat transfer enhancement reduces by intraparticle porosity after $\varepsilon_p = 0.3$ for high Reynolds number. Figure 9 shows that the rate of heat transfer increases with an increase of intraparticle porosity for the low values of Re number (i.e. Re = 50). However, for high values or Re number (i.e. Re = 600), there is an optimum value for intraparticle porosity in which maximum heat transfer enhancement occurs. For the considered problem, it seems that for $\varepsilon_f = 0.4$ and $\varepsilon_f = 0.6$, the maximum heat transfer enhancement occurs around $\varepsilon_p = 0.3$ (around 300 per cent) for Re = 600, 450 and 250. However, for $\varepsilon_f = 0.75$, the maximum heat transfer enhancement is observed at $\varepsilon_p = 0.6$ for Re = 600 and 450. The enhancement of heat transfer with dual scale porous media seems very ac\attractive compared with other passive heat transfer enhancement methods (such as Manca *et al.*, 2011, Kalidasan *et al.*, 2018, Pop *et al.*, 2017).

Figure 10 is prepared to show the change of overall heat transfer enhancement with Re, inter and intraparticle porosity. The comparison of the ratio of heat transfer enhancement and the increase of pressure drop between a dual scale and mono-scale porous media with governing parameters are presented. The $(Nu^*/Nu_o)/(f/f_o)$ ratio of shows the change of overall performance of heat transfer in a porous medium by using intraparticle voids. As intraparticle channels are provided inside the particles, heat transfer considerably increases; however; the pressure drop through the porous media does not change or only a comparatively smaller increase exists. For instance, a porous medium with $\varepsilon_p = 0.4$, the opening of channel with an intrinsic porosity of $\varepsilon_p = 0.4$ can enhance heat transfer by 300 per cent with almost no change of pressure drop. Figure 10 also shows that the overall performance of heat transfer enhancement depends on Reynolds number and intraparticle size. By increasing the Reynolds number and intraparticle porosity, the overall performance of heat transfer enhancement increases for the studies range of the governing parameters.

6. Conclusion

Fluid flow and heat transfer in a dual scale two-dimensional porous media consisting of square rods were investigated, numerically. The continuity, Navier–Stokes and energy equations both for intra and interparticle pores and entire REV of dual scale porous media were solved. The present study revealed that the intraparticle porosity plays an important role in heat transfer through a dual scale porous medium. Based on the obtained results and the performed discussion, following observations can be concluded:

(1) Heat transfer rate in a porous media increases with the inserting pores in the particle in the flow direction. The enhancement of heat transfer by inserting intraparticle pores is very interesting and attain to 300 per cent if it is compared with the mono-scale porous media.

(2) The rate of increase of heat transfer rate by inserting intraparticle pores depends on Reynolds number and intraparticle porosity. Generally, for low values of intraparticle porosity (such as $\varepsilon_p = 0.2$) heat transfer rate increases with Re number and intraparticle porosity. However, for large values of intraparticle porosity (such as $\varepsilon_p = 0.4$) the heat transfer enhancement may slightly decrease with the increase of intraparticle porosity. The rate of decrease depends on the interparticle porosity and Reynolds number.

(3) For the porous media with low values of interparticle porosity (i.e. $\varepsilon_f = 0.4$), an optimum intraparticle porosity exists for which the highest heat transfer enhancement can be achieved. This value was found around 0.3 ($\varepsilon_p = 0.3$) when the interparticle porosity is 0.4 (i.e. $\varepsilon_f = 0.4$).

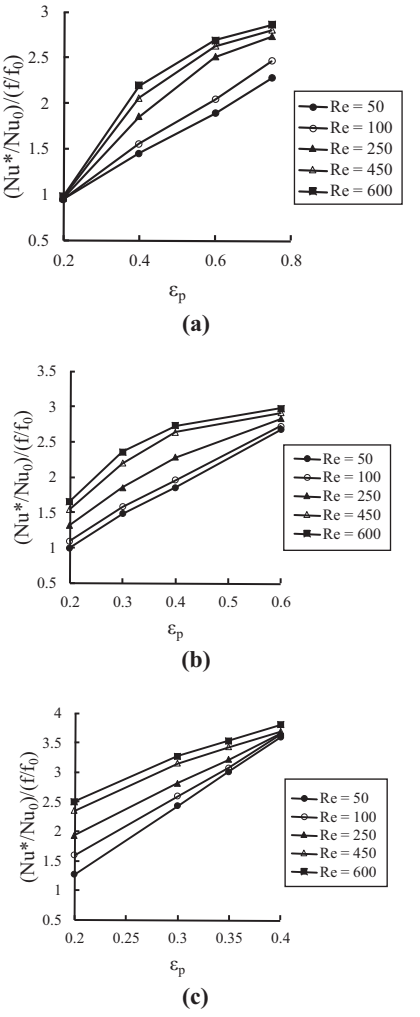

Figure 10.
The overall performance of heat transfer and pressure drop with intraparticle porosity for different values of interparticle porosity and Reynolds number

(4) The overall performance of heat transfer enhancement by providing interparticle pores in the flow direction in particles is high, particularly for porous media with low values of interparticle porosity (i.e. $\varepsilon_f = 0.4$). Heat transfer can be enhanced by 300 per cent without changing of pressure drop if proper intraparticle pores in flow direction are provided.

As can be seen, the results of the study are very interesting especially from heat transfer enhancement point of view. However, further studies are required. For instance, studies should be performed to analyzed the rate of the heat transfer enhancement for different shapes and arrangements of particles and a wider range of porosity. The other important parameter influencing heat transfer enhancement is the direction of pores. In the present study, the intraparticle pores are in flow direction, hence the enhancement rate of heat transfer for different directions of pores must also be investigated.

References

Celik, H., Mobedi, M., Manca, O. and Ozkol, U. (2017), "A pore scale analysis for determination of interfacial convective heat transfer coefficient for thin periodic porous media under mixed convection", *International Journal of Numerical Methods for Heat and Fluid Flow*, Vol. 27, pp. 2775-2798.

Gamrat, G., Favre-Marinet, M. and Le Person, S. (2008), "Numerical study of heat transfer over banks of rods in small reynolds number cross-flow", *International Journal of Heat and Mass Transfer*, Vol. 51 Nos 3/4, pp. 853-864.

Ingham, D.B. and Pop, I. (2005), *Transport Phenomena in Porous Media III*, Elsevier, Great Britain.

Kalidasan, K., Velkennedy, R., Taler, J., Taler, D., Oclon, P. and Rajesh, K.P. (2018), "Numerical study of air convection in a rectangular enclosure with two isothermal blocks and oscillating bottom wall temperature", *International Journal of Numerical Methods for Heat and Fluid Flow*, Vol. 28 No. 1, pp. 103-117.

Kuwahara, F., Shirota, M. and Nakayama, A. (2000), "A numerical study of interfacial convective heat transfer coefficient in two-energy equation model for convection in porous media", *International Journal of Heat and Mass Transfer*, Vol. 44 No. 6, pp. 1153-1159.

Manca, O., Nardini, S. and Ricci, D. (2011), "Numerical investigation of air forced convection in channels with differently shaped transverse ribs", *International Journal of Numerical Methods for Heat and Fluid Flow*, Vol. 21 No. 5, pp. 618-639.

Ozgumus, T. and Mobedi, M. (2014), "Effect of pore to throat size ratio on interfacial heat transfer coefficient of porous media", *Journal of Heat Transfer*, Vol. 137 No. 1, p. 012602

Penha, D.L., Geurts, B., Stolz, S. and Nordlund, M. (2011), "Computing the apparent permeability of an array of staggered square rods using volume-penalization", *Computers and Fluids*, Vol. 51 No. 1, pp. 157-173.

Pop, I., Sheremet, M. and Cimpean, D.S. (2017), "Natural convection in a partially heated wavy cavity filled with a nanofluid using buongiorno's nanofluid model", *International Journal of Numerical Methods for Heat and Fluid Flow*, Vol. 27 No. 4, pp. 924-940.

Saito, M.B. and de Lemos, M.J.S. (2005), "Interfacial heat transfer coefficient for non-equilibrium convective transport in porous media", *International Communications in Heat and Mass Transfer*, Vol. 32 No. 5, pp. 666-676.

Sabet, S. and Mobedi, M. (2016), "A pore scale study on fluid flow through Two-Dimensional dual scale porous media with small number of intraparticle pores", *Polish Journal of Chemical Technology*, Vol. 18 No. 1, pp. 80-92.

Yu, B. and Cheng, P. (2002), "A fractal permeability model for Bi-dispersed porous media", *International Journal of Heat and Mass Transfer*, Vol. 45 No. 14, pp. 2983-2993.

Further reading

Nakayama, A. (1995), *PC-Aided Numerical Heat Transfer and Convective Flow*, CRC Press.

Corresponding author

Moghtada Mobedi can be contacted at: moghtadamobedi@iyte.edu.tr